Analytical method for designing grating-compensated dispersion-managed soliton systems

Y. H. C. Kwan, K. Nakkeeran, and P. K. A. Wai

Photonics Research Centre and Department of Electronic and Information Engineering, The Hong Kong Polytechnic University, Hung Hom, Hong Kong

Manuscript received May 26, 2003; revised manuscript received October 13, 2003; accepted December 3, 2003

We present a useful analytical method for designing grating-compensated dispersion-managed (DM) soliton systems for any desired input pulse widths and energies. The pulse-width and chirp evolution equations derived from the variational method are solved exactly to obtain the explicit analytical expressions for the length of the dispersion map and the grating dispersion. We also extend our analytical method to design grating-compensated DM soliton systems with loss and gain. We show that our analytically designed DM soliton systems also apply even if the chirped fiber gratings have group-delay ripples. The results obtained from our analytical method are in good agreement with those obtained from full numerical simulations. Finally a 160-Gbits/s transmission system is simulated with all the important higher-order effects to show the effectiveness of our analytical design.

OCIS codes: 060.4510, 220.4830.

1. INTRODUCTION

Growth of Internet traffic and e-commerce are demanding high-speed transmission lines. Recent studies have demonstrated that dispersion management is one of the promising techniques for high-speed data transmission in fiber-optic links.[1] Dispersion-compensating techniques utilize compensating elements such as dispersion-compensating fibers (DCFs), optical phase conjugation, and chirped fiber gratings (CFGs). In terrestrial systems, many transmission lines have already been installed under ground, and the cost of upgrading such systems to dispersion-managed (DM) systems is quite expensive. The economic and simple way is to insert lumped dispersion compensators at amplifier locations. CFGs are effective lumped dispersive elements because of their compact sizes, high bandwidth times dispersion figure of merit, the capability to compensate higher-order dispersion, low insertion loss, and the absence of nonlinear effects. It has been shown that solitons exist in DM fiber transmission systems utilizing ideal CFGs for dispersion compensation, and the transmission speed can be up to 100 Gbits/s.[2,3]

Chirped fiber gratings (CFGs), however, have group-delay ripples (GDR) that are the result of imperfections formed during the fabrication of gratings. The GDR induce side peaks in the pulse profile as shown in Fig. 1. In the absence of nonlinearity, the amplitudes of these side peaks grow each time the pulse passes through a CFG. The side peaks cause intersymbol interference and degrade the transmission system performance.[4,5] In CFG-compensated DM soliton systems, the growth of these side peaks is suppressed.[6] For return-to-zero transmission experiments with CFGs as the dispersion compensator, with 10 Gbits/s over 2900 km,[7] 4×10 Gbits/s over 800 km,[8] 16×20 Gbits/s over 400 km,[9] and 40 Gbits/s over 500 km,[10] have already been reported. A design for light traffic conditions at a 40-Gbits/s transmission with CFGs has been investigated by numerical simulations.[11]

The first step to set up any DM soliton system is to design the transmission lines in terms of the dispersion map length, fiber, and pulse parameters. To date, there is no completely analytical method to find soliton solutions for CFG-compensated DM soliton systems. We can, however, obtain the numerical soliton solutions by the commonly used numerical averaging method[12,13] in which the pulse temporal data at two extrema of the slow dynamics in the evolution of the pulse parameter (amplitude or width) during pulse propagation in the DM soliton system are averaged. The averaging procedure is repeated until a stable soliton solution of the DM soliton system is obtained. This numerical averaging technique is widely used in the design of DM soliton systems compensated by DCFs, and it can also be used in DM soliton systems with CFGs as dispersion compensators. The averaging method, however, starts with an arbitrary initial pulse width and energy, and the initial pulse may not converge to a stable soliton solution. It is therefore difficult to obtain a stable solution for the desired pulse width and energy simultaneously. In general, system engineers are interested in designing DM soliton systems for a given bit rate (hence the pulse width) and initial pulse energy from the available laser source. One can use the averaging algorithm to perform a massive study, but the process can be time-consuming.

In addition to the numerical methods, an efficient way to describe the pulse dynamics in a DM soliton system is by variational analysis.[14,15] With a suitable ansatz, one can derive a set of ordinary differential equations (ODEs) governing the evolution of the pulse parameters in DM soliton systems. Typically, the set of coupled ODEs has to be solved numerically. Numerical solutions of these ODEs are not only useful to describe the dynamics of the

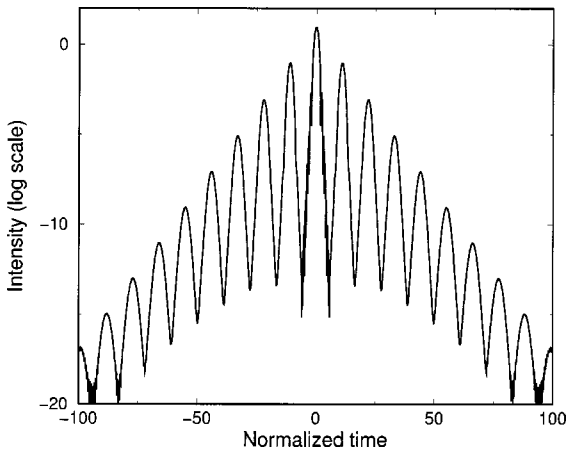

Fig. 1. Temporal pulse profile of solitons in grating-compensated DM soliton systems with GDR.

DM solitons, but also to derive the parameters of the stable DM soliton in any given DM transmission systems. Results can be obtained much faster by this semianalytic method than by full simulations with the numerical averaging method. Nakkeeran *et al.*[16] presented a completely analytical procedure that used a variational approach to design DM soliton systems compensated by DCFs. The length of the fiber segments in a two-step dispersion map can be calculated explicitly for any given pulse (width and energy) and fiber (dispersion and nonlinearity) parameters. They have also shown that the analytical design procedure can be applied to DM soliton systems with loss and gain. Using the variational analysis, Poutrina and Agrawal[17] proposed design guidelines for a given two-step DM soliton system. They can obtain the input pulse width, chirp, and energy for any given dispersion map parameters in DM soliton systems. We have shown that the variational analysis can also be applied to design DM soliton systems compensated by CFGs.[18] For a set of given parameters of a dispersion map in any grating-compensated DM soliton system, the required input pulse widths and energies can be found explicitly from that semianalytical design procedure. We have also shown that, in a CFG-compensated DM soliton system with loss and gain, we can adjust the location of the grating in the dispersion map to a chirp-free position and obtain the desired input pulse parameters for the system.[18] Here, we consider the inverse problem, that is, to find the dispersion map parameters for any given fiber and pulse parameters in such systems.

In this paper we present an efficient analytical method to design the dispersion map for a given pulse (energy and width) and fiber (dispersion and nonlinearity) parameters in any DM soliton communication system compensated by CFGs. The gratings are modeled as lumped dispersion compensators without GDR. Using a Gaussian ansatz in the variational analysis, we derive the pulse evolution equations. Then we obtain the analytical expressions to calculate the grating dispersion and dispersion map length by solving the evolution equations for the given pulse and fiber parameters. We also extend this analytical method to design systems with loss and gain. It is difficult to include the side peaks caused by GDR in the variational analysis. However, because the side peaks do not significantly affect the dynamics of a single DM soliton, our analytical procedure can be used to design DM soliton systems compensated by CFGs with GDR.[6] The results obtained from our analytical method are in good agreement with those obtained with the numerical averaging method even in the presence of GDR in the gratings. Finally, we report the transmission performance of a 160-Gbits/s CFG-compensated DM soliton system designed by the proposed analytical method.

The paper is organized as follows. In Section 2 we derive the expressions of grating dispersion and dispersion map length for given fiber and pulse parameters in lossless DM fiber systems. In Section 3 we extend the design method to a lossy DM fiber system with a map length equal to and shorter than the amplifier spacing. In Section 4 we study the effect of GDR in DM fiber systems. In Section 5 a 160-Gbits/s transmission system is simulated with all the important higher-order effects to show the effectiveness of our analytical design. We draw our conclusion in Section 6.

2. METHOD FOR DESIGNING CHIRPED FIBER GRATING-COMPENSATED LOSSLESS DISPERSION-MANAGED SOLITON SYSTEMS

Nakkeeran *et al.*[16] have considered the ODEs derived from the variational analysis[14,15] of a DCF-compensated DM soliton system. In that study, by solving the ODEs governing the evolution of the pulse width and chirp, the authors derived an analytic expression for the anomalous and normal dispersion fiber lengths in terms of other fiber (group-velocity dispersion and Kerr coefficients) and pulse (energy, minimum, and maximum widths) parameters. Hence one can calculate the required dispersion map length for the periodic evolution of a Gaussian pulse with a given width and energy. Here we use a similar procedure to derive the explicit analytic expressions for the fiber length and grating dispersion in a DM soliton system compensated by CFG.

The dynamics of a pulse propagating in an optical fiber under the influence of the Kerr nonlinearity and periodically varying dispersion is governed by the nonlinear Schrödinger equation:

$$i\frac{\partial \psi}{\partial z} - \frac{\beta(z)}{2}\frac{\partial^2 \psi}{\partial t^2} + \gamma|\psi|^2\psi = 0, \tag{1}$$

where ψ is the slowly varying envelope of the axial electrical field; and z, t, $\beta(z)$, and γ represent the normalized distance, normalized time, group-velocity dispersion, and self-phase modulation parameters, respectively. The group-velocity dispersion parameter $\beta(z) = \beta$ for $z \neq (n + 1/2)L$, where n is an integer and L is the dispersion map length. The gratings are located at $z = (n + 1/2)L$ and their actions are given by the transfer function $F(\omega)$ such that $\psi_{\text{out}}(z, \omega) = F(\omega)\psi_{\text{in}}(z, \omega)$, where ω is the angular frequency and ψ_{in} and ψ_{out} are the pulse spectra before and after the gratings. The CFGs have GDR that are the result of the imperfections in the grating manufacturing processes. The GDR will introduce side peaks in the pulse profile as shown in Fig. 1.[5,6]

It is difficult to include these side peaks in the pulse ansatz of the pulse evolution equations by use of the variational principle. The effect of GDR is to modify the grating dispersion.[6] The ripple period of GDR in CFGs can be as small as 10 pm, which is much shorter than the signal bandwidth in most practical cases. When the signal bandwidth is larger than the ripple period, the effect of GDR is small and the effective grating dispersion is equal to the mean grating dispersion.[6] We therefore neglect the effect of the ripples in the variational analysis. We study the effect of GDR in Section 4. The grating filter transfer function is modeled as

$$F(\omega) = \exp\left(\frac{ig\omega^2}{2}\right), \tag{2}$$

where g is the average lumped dispersion of the grating.[6]

Equations (1) and (2) can be solved by the variational method. We choose a Gaussian ansatz:

$$q(z, t) = x_1 \exp\left\{-\frac{(t - x_2)^2}{{x_3}^2} + i\left[\frac{x_4(t - x_2)^2}{2} + x_5(t - x_2) + x_6\right]\right\}, \tag{3}$$

where x_1, x_2, x_3, x_4, x_5, and x_6 depend on z and correspond to the amplitude, temporal position, width, quadratic phase chirp, center frequency, and phase, respectively, of the pulse. The evolution of the pulse-width and chirp parameters in the optical fibers is given by the following coupled equations:

$$\frac{dx_3}{dz} = -\beta x_3 x_4, \tag{4}$$

$$\frac{dx_4}{dz} = \beta\left({x_4}^2 - \frac{4}{{x_3}^4}\right) - \frac{\sqrt{2}\gamma E_0}{{x_3}^3}, \tag{5}$$

where $E_0 = {x_1}^2 x_3$ is a constant proportional to the energy of the Gaussian pulse. In this design procedure we consider that the pulse is launched at the midpoint of the fiber segment, where the DM soliton has the minimum pulse width ($x_{3\min}$). When the DM soliton reaches the end of the fiber segment, the pulse breathes to the maximum pulse width ($x_{3\max}$) and there the pulse will enter the CFG for dispersion compensation.

To model the effect of the CFG, we exactly solve Eq. (1) by setting the nonlinear coefficient $\gamma = 0$ for a length of fiber l. Then we take the fiber length to zero while keeping the total dispersion $\int_0^l \beta(z)dz = g$ constant. That is, we model a CFG as a segment of an ideal fiber with zero length and finite dispersion. The effects of CFG on pulse width and chirp are given by

$$\begin{aligned} {x_{3\text{out}}}^2 &= {x_{3\text{in}}}^2 H, \\ x_{4\text{out}} &= \frac{1}{H}\left[x_{4\text{in}} - g\left({x_{4\text{in}}}^2 + \frac{4}{{x_{3\text{in}}}^4}\right)\right], \\ H &= g^2\left({x_{4\text{in}}}^2 + \frac{4}{{x_{3\text{in}}}^4}\right) - 2g x_{4\text{in}} + 1, \end{aligned} \tag{6}$$

where y_{in} and y_{out} represent the values of the parameter y at the input and the output of the grating.

Our aim is to derive explicit analytical expressions for the length of the fiber segment and the grating dispersion in terms of the fiber dispersion coefficient (β), Kerr coefficient (γ), maximum pulse width ($x_{3\max}$), minimum pulse width ($x_{3\min}$), and pulse energy (E_0). This can be achieved when we solve Eqs. (4)–(6). Taking the derivative of Eq. (4) with respect to z and using Eq. (5), we obtain the equation for pulse duration as

$$\frac{d^2x_3}{dz^2} = \frac{4\beta^2}{{x_3}^3} + \frac{\sqrt{2}\beta\gamma E_0}{{x_3}^2}. \tag{7}$$

Integrating Eq. (7) with respect to x_3, we obtain

$$\frac{1}{2}\left(\frac{dx_3}{dz}\right)^2 = \frac{-2\beta^2}{{x_3}^2} - \frac{\sqrt{2}\beta\gamma E_0}{x_3} + c. \tag{8}$$

The constant of integration c can be evaluated directly at the midpoint of the fiber where the pulse duration reaches its minimum ($x_{3\min}$) as

$$c = \frac{2\beta^2}{{x_{3\min}}^2} + \frac{\sqrt{2}\beta\gamma E_0}{x_{3\min}}. \tag{9}$$

The DM soliton breathes to the maximum pulse width $x_{3\max}$ at the input of the grating, i.e., $x_{3\text{in}} = x_{3\max}$. From Eq. (4), we have $x_{4\text{in}} = -\dot{x}_{3\max}/(\beta x_{3\max})$, where $\dot{x}_{3\max}$ is the derivative of x_3 with respect to z at $x_3 = x_{3\max}$. Then, using Eq. (8), we can express $x_{4\text{in}}$ as

$$x_{4\text{in}} = \frac{-1}{\beta x_{3\max}}\left(\frac{-4\beta^2}{{x_{3\max}}^2} - \frac{2\sqrt{2}\beta\gamma E_0}{x_{3\max}} + 2c\right)^{1/2}. \tag{10}$$

In deriving Eq. (10) we used the positive root of $\dot{x}_3$ from Eq. (8) because the pulse width is increasing from the minimum ($x_{3\min}$) at the midpoint of the fiber to the maximum ($x_{3\max}$) at the input of the grating. The function of the grating is to reverse the input chirp while preserving the same input pulse width, i.e., $x_{4\text{out}} = -x_{4\text{in}}$ and $x_{3\text{out}} = x_{3\text{in}}$. From Eqs. (6), the grating will reverse the chirp of the soliton without changing its width if $H = 1$. With this condition, we obtain the expression for the grating dispersion as

$$g = \frac{2{x_{3\max}}^4 x_{4\text{in}}}{4 + {x_{3\max}}^4 {x_{4\text{in}}}^2}. \tag{11}$$

Integrating Eq. (8) with respect to z, we find the length of the fiber to be

$$L = 2G - \frac{\gamma\beta E_0 \ln(4c x_{3\min} - 2\sqrt{2}\gamma\beta E_0)}{c\sqrt{c}}, \tag{12}$$

where

$$G = [\sqrt{cA} + \gamma\beta E_0 \ln(2\sqrt{2cA} + 4cx_{3\max} - 2\sqrt{2}\gamma\beta E_0)]/(2c\sqrt{c}),$$

$$A = 2c{x_{3\max}}^2 - 2\sqrt{2}\beta\gamma E_0 x_{3\max} - 4\beta^2.$$

For a given fiber dispersion (β), Kerr nonlinearity (γ), minimum pulse width ($x_{3\min}$), maximum pulse width ($x_{3\max}$), and pulse energy (E_0), we can obtain the grating dispersion (g) and fiber length (L) from Eqs. (11) and (12), respectively.

The maximum pulse width ($x_{3\max}$) is not a commonly used parameter to describe the property of a DM soliton system. Recently, it has been reported that the maximum pulse width is related to the map strength, which is an important parameter that describes the property of a DM soliton system.[19] The map strength S is defined as

$$S = \frac{|L\beta - g|}{{\tau_0}^2}, \tag{13}$$

where $\tau_0 = \sqrt{2}\ln 2 x_{3\min}$ is the full width at half-maximum (FWHM) intensity pulse width. The relation between the maximum pulse width ($x_{3\max}$) and map strength (S) is

$$x_{3\max} = \left(\frac{R|L\beta - g|}{S}\right)^{1/2}, \tag{14}$$

where $R = {x_{3\max}}^2/{\tau_0}^2$ is the breathing parameter. The breathing of the pulse increases as the map strength increases. It has been proved that, around the map strength value of $S \approx S_0 = 1.65$, the pulse breathing parameter R equals S_0.[19] Using this relationship in Eq. (14) and then in Eq. (13), it has been derived that the maximum and minimum pulse widths of any DM soliton systems with a map strength of 1.65 are related as

$$x_{3\max} = (1.65)^{1/2}\tau_0 = (1.65 \times 2\ln 2)^{1/2} x_{3\min}. \tag{15}$$

Hence, to analytically design a dispersion map with map strength $S \approx 1.65$, we need only the minimum pulse width ($x_{3\min}$) and energy (E_0) as input pulse parameters. The maximum pulse width ($x_{3\max}$) can be calculated from Eq. (15). Also, to design a dispersion map with map strength $S < 1.65\,(S > 1.65)$, we have to consider

$$x_{3\max} < (1.65 \times 2\ln 2)^{1/2} x_{3\min}[x_{3\max} > (1.65 \times 2\ln 2)^{1/2} x_{3\min}].$$

To illustrate the effectiveness of our analytical design procedure for lossless DM soliton systems, we use the results obtained from our analytical design procedure as initial conditions for the averaging method[13] to find the numerical periodic DM soliton solutions. We find that the numerical soliton solutions of the nonlinear Schrödinger equation in general converge to the same pulse width that we used to analytically design the dispersion map. We also checked the stability of the numerical soliton solutions by propagating them over 100,000 km.

We consider a fiber dispersion of 1 ps/(km nm), a nonlinearity of 2 $\mathrm{km^{-1}\,W^{-1}}$, and an input width of 5 ps (which corresponds to 40-Gbits/s transmission). The maximum pulse widths and energies are shown in Fig. 2. Note that the input pulse width of 5 ps is the FWHM ($\sqrt{2}\ln 2 x_{3\min}$). From Fig. 2, the maximum pulse width drops by less than 10% even when the energy increases almost threefold. We designed the DM soliton systems with map strengths of 1.65 (solid line) and 3 (dashed line) using the appropriate maximum pulse width. Figure 3 shows the grating dispersion and map length values of the dispersion maps calculated from Eqs. (11) and (12), respectively. As the pulse energy increases, the grating dispersion decreases, but the dispersion map length increases, i.e., the anomalous average dispersion of the dispersion map increases so as to balance the increase in the nonlinear effect. The grating dispersions and map lengths are larger for the dispersion map with higher map strength. The input FWHM of the numerical soliton solutions obtained for different energies and map strengths S in the analytically

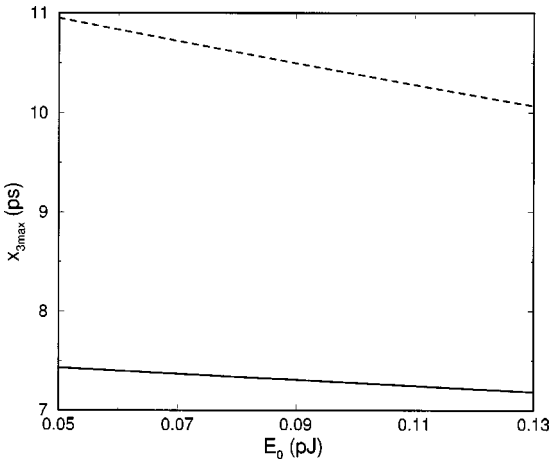

Fig. 2. Maximum FWHMs used in the design of lossless CFG-compensated DM soliton systems for a map strength of 1.65 (solid line) and 3 (dashed line).

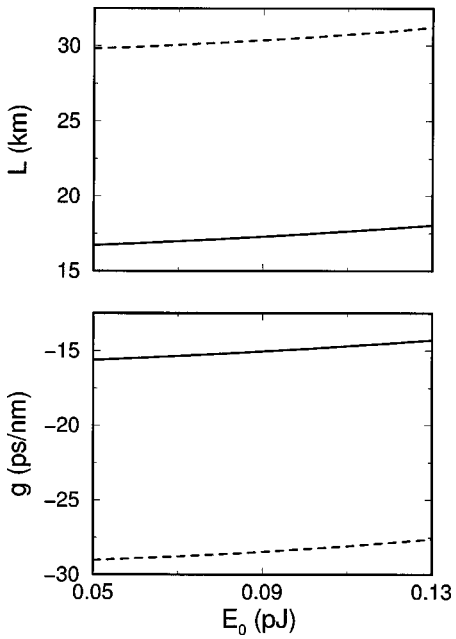

Fig. 3. Grating dispersion (g) and map length (L) obtained by the analytical method for designing lossless CFG-compensated DM soliton systems for a map strength of 1.65 (solid line) and 3 (dashed line).

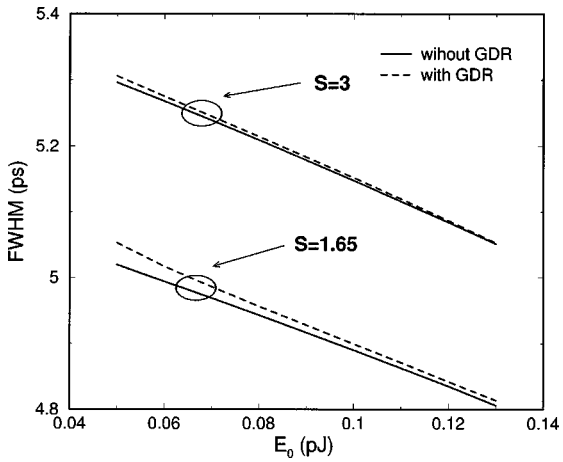

Fig. 4. FWHM of the DM solitons obtained from the numerical averaging method at the middle of the fibers versus pulse energy E_0 for lossless DM soliton systems.

designed DM soliton systems are shown as solid lines in Fig. 4. The numerical results are close to the assumed input pulse width of 5 ps in the systems.

3. METHOD FOR DESIGNING CHIRPED FIBER GRATING-COMPENSATED DISPERSION-MANAGED SOLITON SYSTEMS WITH LOSS AND GAIN

A. Dispersion-Managed Soliton Systems with Amplifier Spacing that is the Same as the Dispersion Map Length

The analytical method to design CFG-compensated lossless DM soliton systems described in Section 2 can be extended to design systems with losses and periodic amplification. In this subsection we elaborate on the analytical procedure to design DM soliton systems with the amplifier spacing equal to the length of the dispersion map. Here we consider a DM soliton system that consists of anomalous dispersion fiber and normal dispersion gratings for dense data packing.[2,3] The same analytical design procedure can also be used to design a DM soliton system that consists of normal dispersion fiber and anomalous dispersion gratings. We assume that the amplifiers are located at the middle of the fiber spans in the dispersion maps because the resulting DM solitons are more stable.[20]

To detail the analytical design procedure for lossy DM soliton systems, we divide the dispersion map into two sections. The first section consists of half of the anomalous dispersion fiber with length $L_{\mathrm{in1}}/2$ followed by half of the grating with dispersion $g_{\mathrm{in1}}/2$ and the second section consists of the other half of the grating with dispersion $g_{\mathrm{in2}}/2$ followed by the remaining half of the fiber with length $L_{\mathrm{in2}}/2$ as shown in Fig. 5(a). The label E_{in1} and E_{in2} are, respectively, the input pulse energies of the first and second sections. It is well known that the average dispersion of the DM soliton system is related to the energy of the DM soliton.[21,22] In the lossless case, the input energy of the DM soliton is available throughout the dispersion map. So the grating at the midpoint of the fiber contributes the same average dispersion to each section of the dispersion map. The same average dispersion is balanced by the same input pulse energy in both sections of the dispersion map. Hence the fiber length in the first section (i.e., the section of the fiber before the grating) and the second section (i.e., the section of the fiber after the grating) of the dispersion map is the same and equal to $L/2$ where L is the dispersion map length. In the presence of losses, the input pulse energy decays exponentially. The average energy available in the second section of the dispersion map is less than that in the first section. It is therefore necessary to adjust the average dispersion of the two sections of the dispersion map according to the locally available average pulse energy in lossy DM soliton systems. This can be done when we shift the location of the grating in such a way that the local average dispersion before and after the grating follows the decrease in the pulse energy.

The analytical design of these two sections of the lossy dispersion map is achieved by the following two-step procedure:

(i) Calculate the fiber length and grating dispersion values of each section by use of the desired pulse and fiber parameters as in a lossless system. Note that the input energy of the pulse used for the second section is the remaining energy after the optical losses in the first section.

(ii) Adjust the average dispersion of each section by means of modifying the grating dispersion such that the ratio between the energy and the average dispersion of the respective section are the same.

For the first section, we calculate the grating dispersion g_{in1} and fiber length L_{in1} as a lossless case using Eqs. (11) and (12), respectively, with the given input pulse energy (E_{in1}), minimum pulse width ($x_{3\mathrm{min}}$), and maximum pulse width ($x_{3\mathrm{max}}$) or the map strength (S) value. Hence the average dispersion of the first section of the dispersion map will be $\beta_{\mathrm{a1}} = (g_{\mathrm{in1}} + L_{\mathrm{in1}}\beta)/L_{\mathrm{in1}}$. The average pulse energy in the first section with length $L_{\mathrm{in1}}/2$ of the lossy system will be

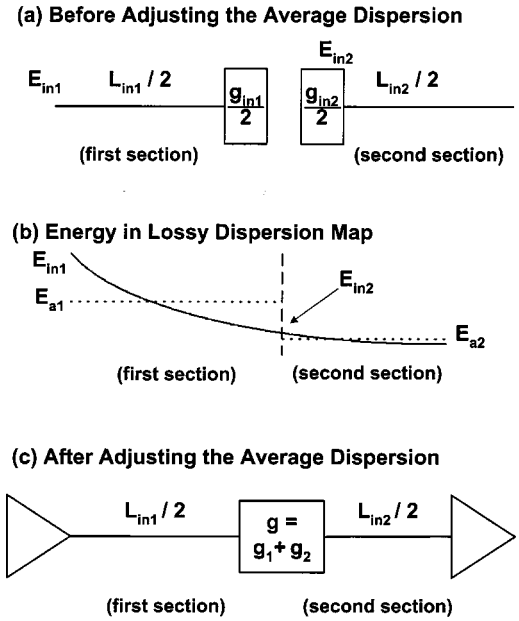

Fig. 5. Schematic of grating-compensated DM soliton systems with the dispersion map length equal to the amplifier spacing.

$$E_{a1} = \frac{1}{(L_{in1}/2)} \int_0^{L_{in1}/2} E_{in1} \exp(-\alpha z) \mathrm{d}z, \qquad (16)$$

where α is the loss coefficient of the fiber. Because of the power loss in the fibers, the input pulse energy will not be available for the pulse dynamics throughout a section of fiber. Figure 5(b) shows the available pulse energy along the dispersion map. The dotted lines are the average energy in each section. Thus the average dispersion of the first section should be decreased accordingly. This can be achieved when we appropriately modify the value of the grating dispersion. To achieve this, we keep the ratio between the average pulse energy and the average local dispersion in the first section the same for both the lossless and the lossy case:

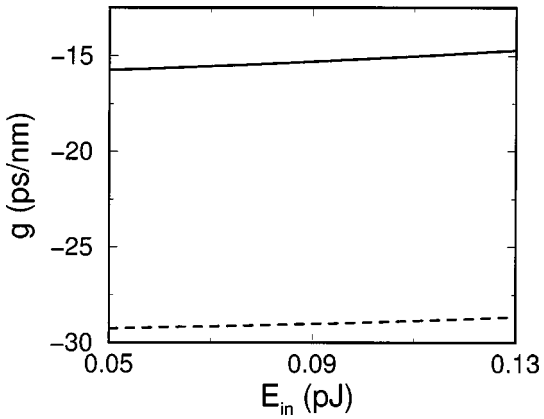

Fig. 6. Grating dispersion (g) obtained by the analytical method for the design of lossy CFG-compensated DM soliton systems with the amplifier spacing equal to the map length for $S = 1.65$ (solid line) and 3 (dashed line).

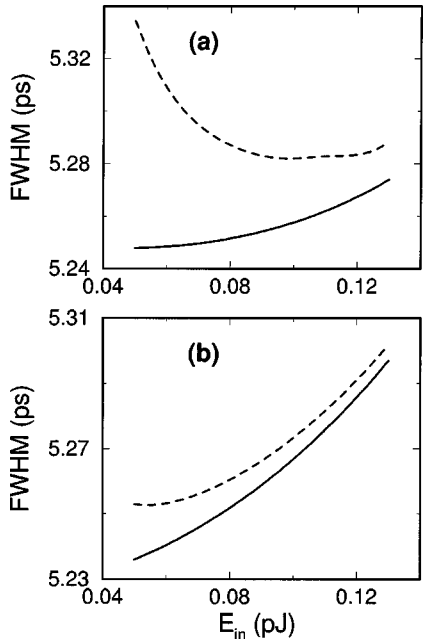

Fig. 7. FWHM of the solitons at the beginning of the dispersion maps versus pulse energy E_{in} for lossy DM soliton systems. Map strength of (a) 1.65 and (b) 3. Solid and dashed curves represent the results obtained in the designed DM soliton systems without and with GDR in the gratings, respectively.

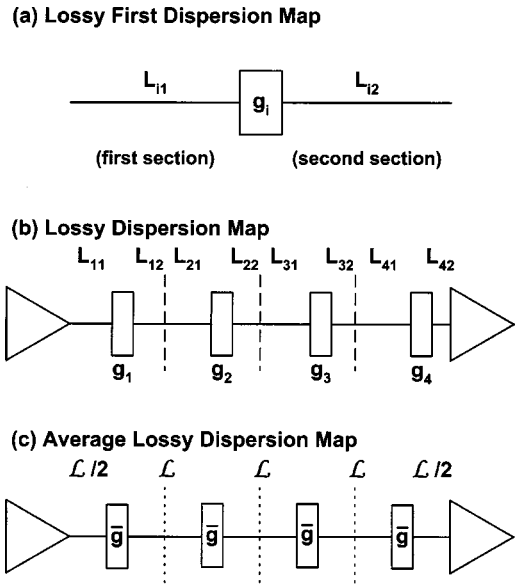

Fig. 8. Schematic of grating-compensated DM soliton systems with the dispersion map length shorter than the amplifier spacing. The grating dispersion $\bar{g}$ is $\Sigma_{i=1}^{4} g_i/4$ and the fiber length $\mathcal{L}$ is $\Sigma_{i=1}^{4}(L_{i1} + L_{i2})/4$.

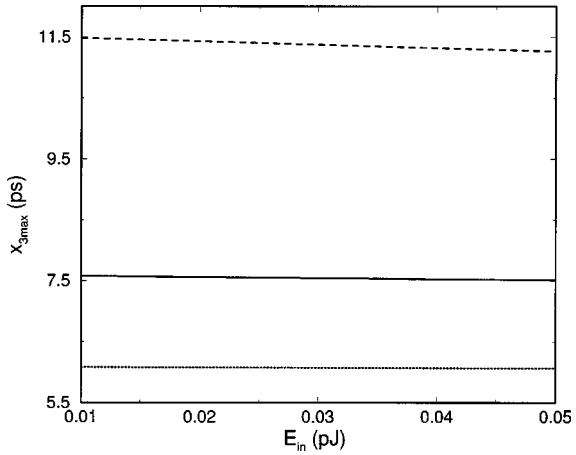

Fig. 9. Maximum FWHMs used in the design of lossy CFG-compensated DM soliton systems for a map strength of 1 (dotted line, lower), 1.65 (solid line), and 3 (dashed line).

$$\frac{E_{in1}}{\beta_{a1}} = \frac{E_{a1}}{\beta_{a1}'} \qquad (17)$$

where E_{in1} is the input pulse energy in the lossless case and β_{a1}' is the average dispersion in the lossy case. Thus the new modified grating dispersion of the first section of the dispersion map $g_1 = (L_{in1}/2)(\beta_{a1}' - \beta)$.

We follow the same procedure in the second section of the dispersion map. The pulse energy at the beginning of the second section is $E_{in2} = E_{in1} \exp[-\alpha(L_{in1}/2)]$. Here we did not include any splicing losses, but one can include the splicing losses and calculate the input pulse energy available for the second section of the dispersion map. The grating dispersion ($g_{in2}/2$) and map length ($L_{in2}/2$) in the second section can be calculated with Eqs. (11) and (12) from the pulse energy (E_{in2}), the same minimum

pulse width ($x_{3\min}$), and the maximum pulse width ($x_{3\max}$). Hence the average dispersion of the second section under the lossless assumption will be $\beta_{a2} = (g_{in2} + \beta L_{in2})/L_{in2}$. Considering the fiber length of the second section to be $L_{in2}/2$, we calculate the average energy (E_{a2}) in the lossy second section of the dispersion map as

$$E_{a2} = \frac{1}{(L_{in2}/2)} \int_0^{L_{in2}/2} E_{in2} \exp(-\alpha z) \mathrm{d}z. \qquad (18)$$

We take loss into account by adjusting the average dispersion of the second section. The modified grating dispersion $g_2 = (L_{in2}/2)(\beta_{a2}' - \beta)$, where $\beta_{a2}' = \beta_{a2} E_{a2}/E_{in2}$.

Cascading the two sections will result in the dispersion map of a grating-compensated lossy DM soliton system with the amplifier spacing the same as the dispersion map length. The total length of the dispersion map is $(L_{in1} + L_{in2})/2$ with $L_{in1}/2 > L_{in2}/2$ and a grating dispersion $g = g_1 + g_2$ as shown in Fig. 5(c).

To show the effectiveness of our method in designing grating-compensated lossy DM soliton systems, we repeat the calculations done in Fig. 4 but include a loss of coefficient $\alpha = 0.2$ dB/km. We appropriately chose the $x_{3\max}$ value in the range between 7.42 and 7.11 ps for $S = 1.65$ and 11.09 and 10.36 ps for $S = 3$, respectively. For a map strength of 1.65, the length of the first section ($L_{in1}/2$) and length of the second section ($L_{in2}/2$) are calculated to be in the range of 8.34–8.85 km and 8.28–8.8 km, respectively. For $S = 3$, the values of $L_{in1}/2$ and $L_{in2}/2$ are in the range of 15.16–16.22 km and 14.41–13.94 km, respectively. Figure 6 shows the calculated grating dispersion (g) of the dispersion map. The effect of pulse energy on the grating dispersion and map length in the lossy case are similar to the lossless case. Both the grating dispersion and the map length values are larger in the higher map strength cases. The solid curves in Figs. 7(a) and 7(b) represent the numerical results for a map strength of 1.65 and 3, respectively. The numerical results are within 6% of the targeted pulse width of 5 ps.

DM soliton systems with the map length equal to the amplifier span are useful for low- and moderate-speed optical communications. For high-speed communications, short dispersion maps are needed.[23–25] Hence there will be more than one dispersion map in an amplification span.

B. Dispersion-Managed Soliton Systems with Amplifier Spacing Longer than Dispersion Map Length

Moubissi *et al.* proposed an analytical method to design DM soliton systems compensated by DCFs with many dispersion maps between the amplifiers.[26] For any given pulse width, energy, and fiber dispersion, the fiber lengths in each map can be individually calculated. The lengths of the fiber segments are different for different dispersion maps within each amplification span. Here we extend their method to the design described in Subsection 3.A to obtain dense DM soliton systems with identical dispersion maps. Such systems make implementation easier.

From Fig. 3, the dispersion map length (L) does not vary significantly even for a large variation in the input pulse energy (E_0). Thus, from the first dispersion map length and a given amplification distance, we can estimate the required number of dispersion maps (m) within one amplification span. For each dispersion map, we apply the analytical design procedure described in Subsection 3.A as shown in Fig. 8(a). We then average the dis-

Table 1. Fiber Lengths of the Dispersion Maps[a]

	Map 1		Map 2		Map 3		Map 4		Map 5	
E_{in} (pJ)	L_{11} (km)	L_{12} (km)	L_{21} (km)	L_{22} (km)	L_{31} (km)	L_{32} (km)	L_{41} (km)	L_{42} (km)	L_{51} (km)	L_{52} (km)
$S = 1$										
0.01	4.195	4.187	4.180	4.175	4.170	4.167	4.164	4.161	4.159	4.157
0.02	4.233	4.216	4.202	4.191	4.182	4.174	4.168	4.163	4.159	4.156
0.03	4.274	4.247	4.226	4.209	4.195	4.184	4.174	4.167	4.161	4.155
0.04	4.316	4.279	4.250	4.227	4.208	4.193	4.180	4.170	4.162	4.155
0.05	4.360	4.312	4.275	4.245	4.221	4.202	4.186	4.174	4.163	4.155
$S = 1.65$										
0.01	6.910	6.888	6.873	6.861	6.853	6.847				
0.02	6.965	6.920	6.888	6.865	6.849	6.837				
0.03	7.023	6.953	6.904	6.870	6.845	6.827				
0.04	7.083	6.987	6.920	6.874	6.840	6.817				
0.05	7.146	7.021	6.936	6.877	6.836	6.806				
$S = 3$										
0.01	12.554	12.484	12.446	12.424						
0.02	12.643	12.499	12.422	12.379						
0.03	12.735	12.514	12.397	12.333						
0.04	12.833	12.529	12.372	12.288						
0.05	12.935	12.543	12.346	12.241						

[a] Obtained by the analytical method for designing lossy CFG-compensated DM soliton systems with the amplifier spacing longer than the dispersion map length.

Table 2. Grating Dispersions of the Dispersion Maps[a]

E_{in} (pJ)	Map 1 g_1 (ps/nm)	Map 2 g_2 (ps/nm)	Map 3 g_3 (ps/nm)	Map 4 g_4 (ps/nm)	Map 5 g_5 (ps/nm)
$S = 1$					
0.01	−9.767	−9.775	−9.781	−9.784	−9.787
0.02	−9.719	−9.735	−9.747	−9.754	−9.759
0.03	−9.673	−9.699	−9.716	−9.727	−9.735
0.04	−9.625	−9.662	−9.685	−9.700	−9.711
0.05	−9.577	−9.624	−9.654	−9.674	−9.686
$S = 1.65$					
0.01	−16.163	−16.144	−16.133		
0.02	−16.142	−16.104	−16.083		
0.03	−16.120	−16.063	−16.033		
0.04	−16.095	−16.021	−15.983		
0.05	−16.068	−15.979	−15.932		
$S = 3$					
0.01	−29.486	−29.329			
0.02	−29.543	−29.227			
0.03	−29.600	−29.124			
0.04	−29.658	−29.021			
0.05	−29.714	−28.914			

[a] Obtained by the analytical method for designing lossy CFG-compensated DM soliton systems with the amplifier spacing longer than the dispersion map length.

Table 3. Average Values of Map Length and Grating Dispersion[a]

Energy E_{in} (pJ)	$S = 1$		$S = 1.65$		$S = 3$	
	$\mathcal{L}$ (km)	$\bar{g}$ (ps/nm)	$\mathcal{L}$ (km)	$\bar{g}$ (ps/nm)	$\mathcal{L}$ (km)	$\bar{g}$ (ps/nm)
0.01	8.343	−9.779	13.744	−16.147	24.954	−29.407
0.02	8.369	−9.743	13.775	−16.110	24.971	−29.385
0.03	8.398	−9.710	13.807	−16.072	24.989	−29.362
0.04	8.428	−9.677	13.840	−16.033	25.011	−29.340
0.05	8.459	−9.643	13.874	−15.993	25.032	−29.314

[a] Obtained from our analytical method in lossy CFG-compensated DM soliton systems.

persion map lengths and grating dispersions within an amplifier span to obtain the final map length ($\mathcal{L}$) and grating dispersion ($\bar{g}$), i.e.,

$$\mathcal{L} = \frac{1}{m}\sum_{i=1}^{m} (L_{i1} + L_{i2}), \tag{19}$$

$$\bar{g} = \frac{1}{m}\sum_{i=1}^{m} g_i, \tag{20}$$

where L_{ij}, $i = 1,\ldots, m$ and $j = 1,2$ is the fiber length of the jth section of the ith dispersion map within an amplifier span, and g_i is the grating dispersion of the ith dispersion map. Figures 8(b) and 8(c), respectively, show the schematic diagrams of the intermediate and final grating-compensated lossy DM soliton systems with four dispersion maps between the amplifiers.

As an illustration, we consider the example discussed in Fig. 4 and include a loss with the coefficient $\alpha = 0.2$ dB/km. Here we study three different map strengths: 1, 1.65, and 3. We use the same fiber dispersion value of 1.18 ps/(km nm) for all three map strengths, and the resulting dispersion maps have three different dispersion map lengths. We use different maximum pulse widths for the three different map strengths as shown in Fig. 9. For the same map strength, the pulse undergoes less breathing when the pulse energy increases, i.e., the maximum pulse width decreases because of the increase in the nonlinear effect. Tables 1 and 2 show the fiber lengths and grating dispersions calculated from the analytical method described in Subsection 3.A, respectively. We consider an amplification span of around 40–50 km, so the number of dispersion maps per amplifier span will be 5, 3, and 2 and the amplification distance will be approximately 42, 42, and 50 km, respectively, for the map strengths of 1, 1.65, and 3. Table 3 shows the average map lengths and grating dispersions for the three map strengths. The grating dispersion is slightly reduced when the pulse energy is increased. The magnitude of the grating dispersion is larger for a higher map strength. To check the validity of our analytical method, we use the numerical averaging method to determine the numerical DM soliton solutions using the Gaussian pulse $[x_1 \exp(-t^2/x_{3\min}{}^2)$, where $x_1 = (E_{in}/x_{3\min})^{1/2}]$ as the initial condition. Solid, dotted, and dashed lines in Fig. 10 show the results obtained from the numerical averaging method for map strengths of 1, 1.65, and 3, respectively. The solid and dotted lines are within 3% whereas the dashed line is 9% from the expected value of 5 ps. We note that the difference in accuracy is not due to fewer (two) maps used in an amplifier span. We also considered another design for a map strength of 3 using a fiber dispersion of 2.94 ps/(km nm) that resulted in four dispersion maps per amplifier span. The results are nearly the same as the dashed line in Fig. 10. The reason for the larger deviation in higher map strength is that the Gaussian ansatz is a good approximation to the core of the DM solitons for lower map

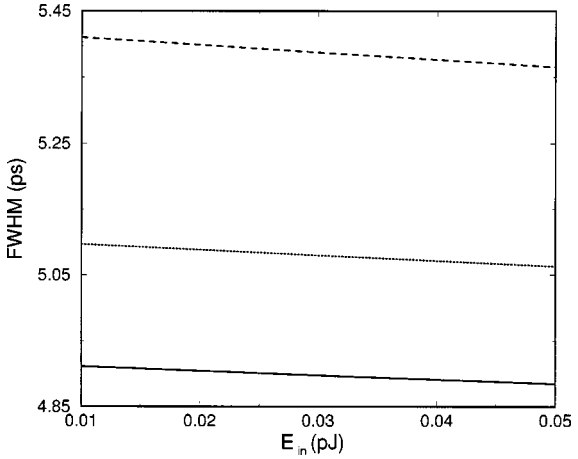

Fig. 10. FWHM of the solitons at the beginning of the dispersion maps versus pulse energy E_{in} for lossy DM soliton systems. Solid (lower), dotted, and dashed lines represent the results for map strengths of 1, 1.65, and 3, respectively.

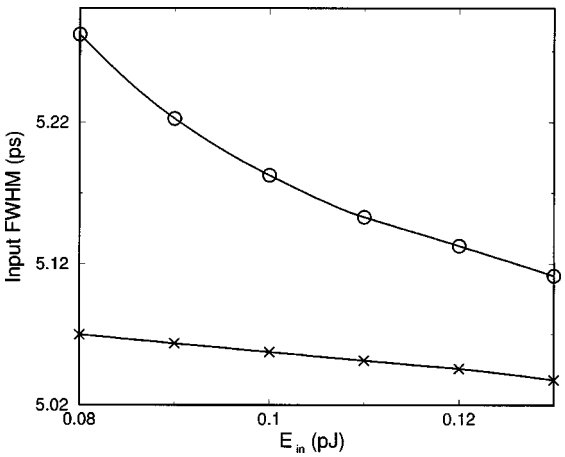

Fig. 11. FWHM of the DM solitons obtained from the numerical averaging method at the beginning of the dispersion maps versus pulse energy E_{in} for lossy DM soliton systems. Crosses and circles are data points for the designed DM soliton system without and with GDR in the gratings, respectively. The ripple amplitude and period of the GDR are 5 ps and 0.064 nm.

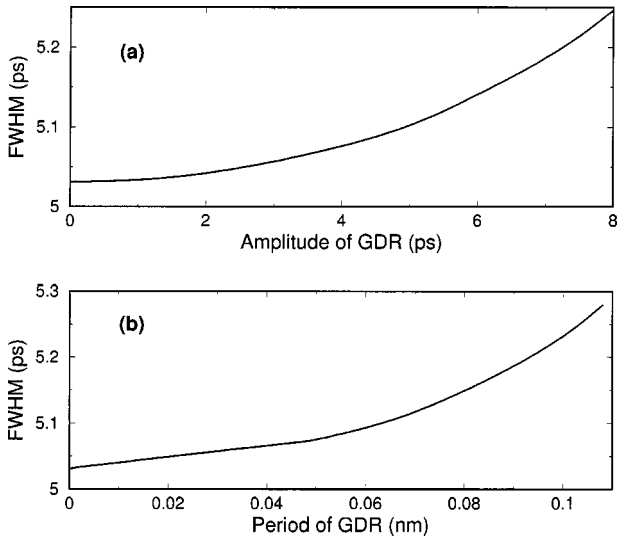

Fig. 12. Effect of GDR in the gratings for lossy DM soliton systems. (a) FWHM of the DM solitons versus ripple amplitude for a constant ripple period of 0.064 nm. (b) FWHM of the DM solitons versus ripple period for a constant ripple amplitude of 5 ps. The pulse energy is 0.13 pJ.

strengths of 1 and 1.65, but not for a high map strength, hence pulse energy.[3,19]

4. EFFECT OF GROUP-DELAY RIPPLES IN CHIRPED FIBER GRATING-COMPENSATED DISPERSION-MANAGED SOLITON SYSTEMS

In the analytical design, we did not consider the GDR in the CFGs and did not include the side peaks in the Gaussian ansatz because of the mathematical complexity. The amplitudes of the side peaks, however, decrease exponentially along the tails of the pulse. The pulse energy mostly concentrates in the central peak rather than the side peaks of the DM solitons. The significance of the side peaks is small for the dynamics of single DM soliton propagation in CFG-compensated DM soliton systems. In general, the structure of the GDR in CFG is quite complex.[27] For simplicity we assume a sinusoidal form of GDR in all the simulations that involve GDR in the gratings.[6] In this section, we first study the effect of GDR on the designed CFG-compensated DM soliton systems for different initial pulse energies. We launch the same Gaussian pulses used in the analytically designed systems but with GDR in the gratings and obtain the DM soliton solutions by the numerical averaging method. We find that the numerical results are in good agreement with the analytical results, except for the cases of large ripple amplitude and period. Finally, we show the evolution of the Gaussian ansatz in the analytically designed system with GDR over 10,000 km. The pulse parameters deviate somewhat from the initial parameters but the core of the pulse remains close to the Gaussian ansatz.

In the absence of loss, we launch the same Gaussian pulse in the analytically designed systems in Section 2. We choose GDR with an amplitude of 5 ps and a period of 0.064 nm in most studied cases. In a real grating, the amplitude can be as low as 1.5 ps and the dominant period is 0.06 nm.[4,27] The dashed lines in Fig. 4 represent the numerical results for GDR. The numerical results in the case of gratings with GDR (dashed lines) are close to that without GDR (solid lines). Thus our analytical method is also useful to design DM soliton systems in the presence of GDR in gratings when loss is negligible.

In lossy DM soliton systems with the map length the same as the amplification distance, we study the effect of GDR in gratings using the same initial Gaussian pulse as that in Subsection 3.A. The dashed curves in Figs. 7(a) and 7(b) show the numerical results obtained by the averaging method for map strengths of 1.65 and 3, respectively. The numerical results are within 6% of the assumed width, 5 ps. Thus the proposed design can be

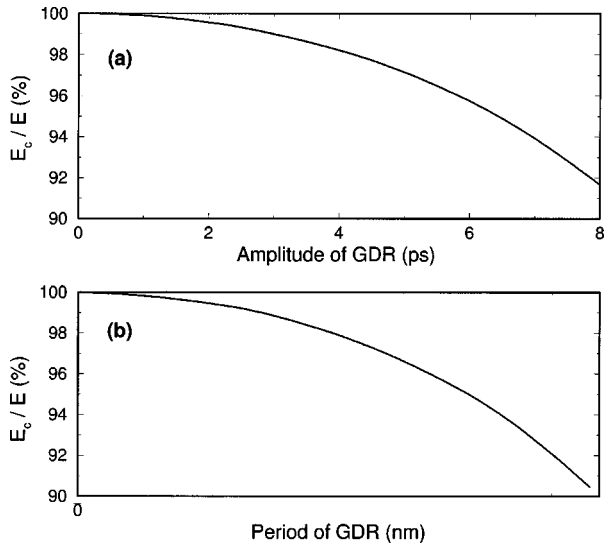

Fig. 13. Effect of ripple period and amplitude of the gratings on the ratio of the energy in the central peak (E_c) to total energy (E) for lossy DM soliton systems. (a) Energy ratio versus ripple period for a constant ripple period of 0.064 nm. (b) Energy ratio versus ripple amplitude for a constant ripple amplitude of 5 ps. The pulse energy is 0.13 pJ.

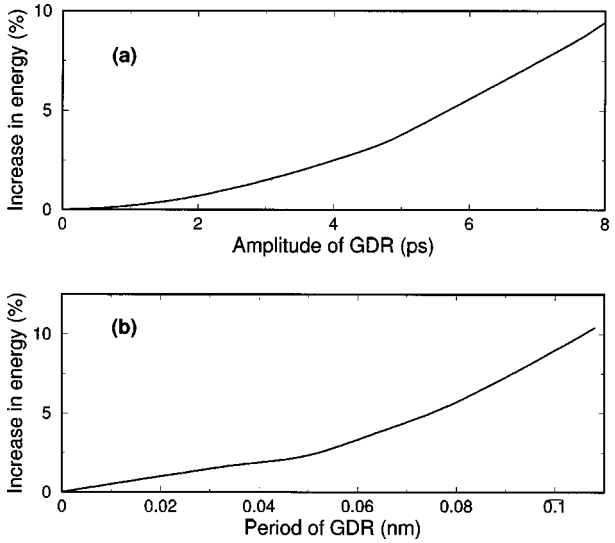

Fig. 14. Effect of GDR in the gratings for lossy DM soliton systems. (a) Percentage of energy difference for a constant ripple period of 0.064 nm. (b) Percentage of energy difference for a constant ripple amplitude of 5 ps. The FWHM of the DM solitons is 5 ps.

applied to lossy systems with GDR when the map length equals the amplification distance.

For the systems with the amplifier spacing longer than the map length, we choose the systems with a map strength of 1.65 where the DM soliton is close to a Gaussian profile.[19] We choose the minimum pulse width to be 5 ps $[(2 \ln 2 x_{3\min})^{1/2}]$ for 40-Gbits/s transmission and the input pulse energies (E_{in}) to range from 0.08 to 0.13 pJ. The fiber dispersion is 1.651 ps/(km nm) and the nonlinearity is 2 $\text{km}^{-1}\text{W}^{-1}$. The different input maximum pulse widths to achieve different input pulse energies are between 7.5 and 7.44 ps. From the analytical design, the map length for these input parameters ranges from 9.91 to 10 km and the grating dispersion ranges from -15.91 to -15.73 ps/nm. We use four dispersion maps so that the amplification distance will be $\sim$40 km.

We then introduce GDR with an amplitude of 5 ps and period of 0.064 nm in the gratings.[6] We launch the Gaussian ansatz $x_1 \exp(-t^2/x_{3\min}{}^2)$, where $x_1 = (E_{\text{in}}/x_{3\min})^{1/2}$ in the analytically designed CFG-compensated DM soliton systems with and without GDR and perform numerical averaging[13] to obtain the stable DM soliton solutions. Figure 11 shows the pulse widths versus pulse energies of the numerical solutions. Crosses and circles are data points corresponding to the cases without and with GDR in the gratings, respectively. The pulse widths of the numerical soliton solutions are close to 5 ps even in the presence of GDR. Because the energy of the side peaks is much smaller than that of the central peak, the change in the pulse width due to the change in the energy of the central peak is small.

Next we study the effect of different ripple amplitudes and periods on our analytically designed CFG-compensated DM soliton systems. We fix the pulse energy (E_{in}) and pulse width ($x_{3\min}$) to be 0.13 pJ and 5 ps, respectively. The ripple amplitude and period are varied from 0 to 8 ps and 0 to 0.11 nm, respectively. Because the ripple amplitude of the GDR can be as low as 1.5 ps and the dominant ripple period is 0.06 nm,[27] we choose the maximum value of the ripple amplitude and period in our study to be 8 ps and 0.11 nm, respectively. The relative phase between the GDR and pulse spectrum is chosen to be π.[6] Figures 12(a) and 12(b) show the pulse widths of the DM solitons versus ripple amplitude and period, respectively. The ripple period and amplitude are kept constant as 0.064 nm and 5 ps in Figs. 12(a) and 12(b), respectively.

We observe that the pulse width of the DM soliton increases when the ripple amplitude or the ripple period increases. For the cases studied, the effective dispersion of the CFGs is almost the same as the grating dispersion because of the small ratio between the ripple period and the pulse spectral bandwidth.[6] As the ripple period or amplitude increases, the energy in the side peaks of the DM soliton increases. Figure 13 shows the ratio between the energy of the central peak (E_c) and that of the whole pulse (E). Thus the nonlinear effect is slightly reduced as more energy is transferred from the central peak to the side peaks resulting in pulse broadening. If we keep the same pulse energy (width), the pulse width (energy) will increase as the ripple amplitude or period increase. The change in pulse width is up to $\sim$6% in Figs. 12(a) and 12(b). For the pulse energy of 0.13 pJ the numerical av-

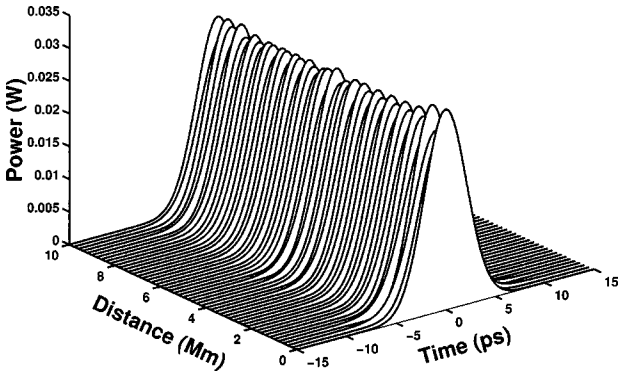

Fig. 15. Evolution of a Gaussian ansatz in the analytically designed CFG-compensated DM soliton system with GDR. The ripple amplitude and period are 5 ps and 0.064 nm, respectively. The pulse shapes are taken just after every five amplifiers.

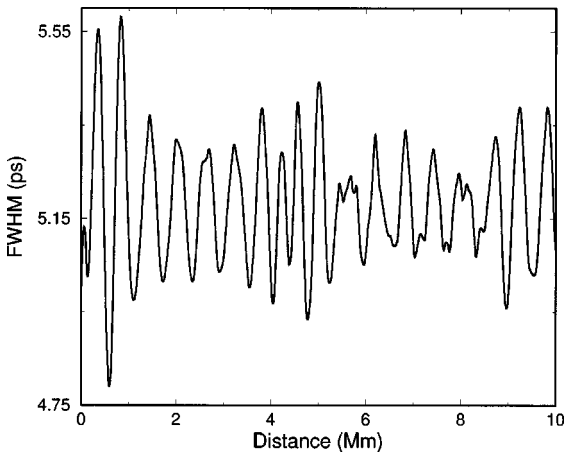

Fig. 16. Slow dynamics of the pulse width of the Gaussian ansatz propagating in the analytically designed DM soliton system with a ripple amplitude of 5 ps and a period of 0.064 nm in CFGs.

eraging method does not give stable DM solitons for a ripple amplitude beyond 8 ps or a ripple period longer than 0.11 nm.

Using the numerical averaging method, we also obtain the pulse energies for a fixed stable input pulse width of 5 ps and different values of ripple amplitude (0–8 ps) and period (0–0.11 nm) in the analytically designed DM soliton system. The energy of the numerical DM soliton for the ideal grating case is ~0.133 pJ at the amplifier location. The required pulse energy increases when the ripple amplitude or period increases. The percentage increase in energy as a function of ripple amplitude and period are shown in Figs. 14(a) and 14(b), respectively. Because of the relative amount of energy in the central peak of the DM soliton decreases as the ripple amplitude or period increases, the DM soliton requires larger energy for the same pulse width. The results demonstrate that our analytical design is effective if the CFGs have small ripple amplitude and short ripple period.

Finally, we study the evolution of the Gaussian ansatz in analytically designed DM soliton systems compensated by CFGs. We choose a Gaussian pulse with a duration of 5 ps (corresponding to 40-Gbits/s transmission) and pulse energy (E_{in}) of 0.13 pJ. For the DM soliton system, we choose a map strength of 1.65, the maximum FWHM as 7.44 ps, and fiber dispersion as 1.65 ps/(km nm). The calculated map length is ~10 km and the grating dispersion is approximately −15.73 ps/nm. We introduce ripples with amplitude and period of 5 ps and 0.064 nm, respectively. The ripple period is chosen as 0.064 nm.[4,27] Figure 15 shows the evolution of the Gaussian pulse over 10,000 km. The pulse core shape does not deviate much from the initial Gaussian profile. The final pulse has a peak intensity of ~29 mW (~30.6 mW for the initial Gaussian pulse) and has side peaks induced by the GDR. The separation between the side peaks is 125 ps and the percentage of the pulse energy transferred to the side peaks of the pulse after propagating for 10,000 km is ~5%. Figure 16 shows the slow dynamics of the pulse width along the propagation distance. The small fluctuations of the pulse width are caused by the interaction between the DM soliton and the dispersive waves because the initial pulse is not an exact DM soliton solution. For comparison the pulse width of the DM soliton solution obtained with the numerical averaging method is ~5.1 ps and has an energy of 0.13 pJ.

5. ANALYTICALLY DESIGNED 160-GBITS/S DISPERSION-MANAGED FIBER SYSTEM PERFORMANCE WITH HIGHER-ORDER EFFECTS

To show the effectiveness of our analytical design for practical DM soliton systems we examine the evolution of a 32-bit pseudorandom sequence in a single channel at 160 Gbits/s over 8000 km. We consider a fiber dispersion of 1 ps/(km nm), a nonlinearity of 2 $\mathrm{km}^{-1}\,\mathrm{W}^{-1}$, an input pulse width of 1.25 ps, and energy (E_{in}) of 0.03 pJ. We choose the map strength to be 1.65 for minimum pulse interaction, which corresponds to a maximum FWHM of 1.9 ps. Using these input parameters in Eq. (12) we calculate the lossless dispersion map length L as 1.02 km. The loss coefficient of fibers is 0.2 dB/km. We consider an amplification span of around 40 km, so the number of dispersion maps between amplifiers will be 40. Thus the final map length ($\mathcal{L}$) and grating dispersion ($\bar{g}$) are calculated with Eqs. (19) and (20) as 1.012 km and −1 ps/nm, respectively. The amplifier noise figure is considered to be 4.5 dB. We use 50 sets of random sequences for both bit sequence and amplifier noise. For high-speed transmission, we include the third-order dispersion of 0.1 ps^3/km and $-0.1\ \mathrm{ps}^3$ in the fiber and the grating sections, respectively. The third-order dispersion of the grating is considered in such a way as to compensate the third-order dispersion in fibers.[28] We also include the intrapulse Raman scattering with the response time of 3 fs.[29] A Gaussian filter with a bandwidth of 1.6 THz whose central frequency is upshifted by 18.3 GHz is placed after each amplifier to reduce the timing jitter and suppress the soliton self-frequency shift.[30] Each amplifier has a gain of 8.2 dB to compensate the power loss in fibers and filter. Figure 17(a) shows the intensity (solid) and timing (dashed) Q factors along the propagation distance. The Q factors are derived in linear units for which the value $Q = 6$ (dotted line) corresponds to a bit-error ratio of 10^{-9}. The timing detection window is chosen to be 70% of the bit window. The eye diagram of a random sequence after 7400 km of transmission at which $Q = 6$ is shown in Fig. 17(b). Figures 7(a) and 7(b) show an excellent performance over transoceanic distance with the analytically designed grating-compensated DM soliton systems. Moreover, it demonstrates the utility of our analytical design in high-speed long-haul CFG-compensated optical fiber transmission systems.

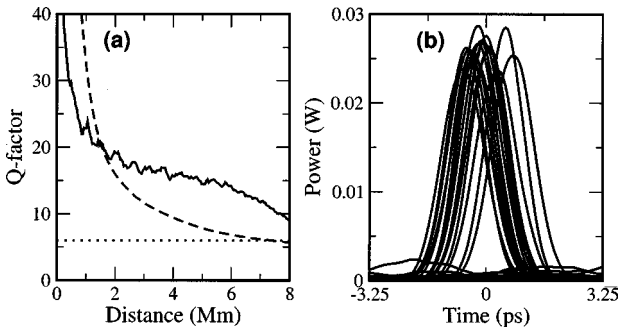

Fig. 17. (a) Intensity (solid curve) and timing (dashed curve) Q factors versus propagation distance. The dotted line shows the value of $Q = 6$. (b) Eye diagram of a particular random sequence after 7400 km.

6. DISCUSSION AND CONCLUSION

The results obtained in this paper will be valid in all cases where the Gaussian ansatz is a good approximation for the soliton solutions of the DM systems compensated by CFGs.[15,19] For a large map strength (>4) or systems with large energy soliton solutions (>0.2 pJ), the Gaussian ansatz is not a good approximation and we find a large deviation between the analytical results and the numerical results. We also observed that the effect of ripples decreases with the pulse width because the ratio

of spectral bandwidth to ripple period increases with the spectral bandwidth for a fixed ripple period.

In this paper we have used anomalous dispersion fiber and a normal dispersion grating because one can pack the signal closer in such systems.[31] Our analytical method can be applied to design DM soliton systems consisting of normal dispersion fibers and anomalous dispersion gratings as well. Finally, the design is not limited to CFGs; it can be used for any dispersion compensators that have lump dispersion, without nonlinearity and power loss.

In conclusion, we have presented an analytical method for designing grating-compensated DM soliton systems. We have explicitly derived the expressions for dispersion map length and grating dispersion by solving the evolution equations of pulse width and chirp obtained from the variational analysis. Using our design method, one can obtain the map length and grating dispersion for the desired bit rate, pulse energy, and fiber dispersion. We have also described the analytical procedures to design lossy DM soliton systems having a dispersion map length equal to or shorter than the amplifier spacing. The results obtained from our analytical design methods are in good agreement with that from the numerical averaging method even in the presence of GDR. The evolution of the Gaussian pulse used in the analytically designed DM soliton system shows little deviation over transoceanic distance. Thus our design procedure is a useful tool to design CFG-compensated DM soliton systems even with GDR. The effectiveness of our analytical method has been supported by the good transmission system performance of the analytically designed 160-Gbits/s CFG-compensated DM soliton system.

ACKNOWLEDGMENT

The authors acknowledge support from the Hong Kong Polytechnic University (project G-YW85).

REFERENCES

1. V. E. Zakharov and S. Wabnitz, *Optical Solitons: Theoretical Challenges and Industrial Perspectives* (Springer, Berlin, Germany, 1998).
2. S. Kumar and A. Hasegawa, "Quasi-soliton propagation in dispersion-managed optical fibers," Opt. Lett. **22**, 372–374 (1997).
3. V. K. Mezentsev and S. K. Turitsyn, "Solitons with Gaussian tails in dispersion-managed communication systems using gratings," Phys. Lett. A **237**, 37–42 (1997).
4. S. G. Evangelides, N. S. Bergano, and C. R. Davidson, "Intersymbol interference induced by delay ripple in fiber Bragg gratings," in *Optical Fiber Communication Conference*, Vol. 4 of 1999 OSA Technical Digest Series (Optical Society of America, Washington, D.C., 1999), pp. 5–7.
5. C. Scheerer, C. Glingener, G. Fischer, M. Bohn, and W. Rosenkranz, "System impact of ripples in grating group delay," in *1999 International Conference on Transparent Optical Networks* (Institute of Electrical and Electronics Engineers, New York, 1999), pp. 33–36.
6. Y. H. C. Kwan, P. K. A. Wai, and H. Y. Tam, "Effect of group-delay ripples on dispersion-managed soliton communication systems with chirped fiber gratings," Opt. Lett. **26**, 959–961 (2001).
7. E. Yamada, T. Imai, T. Komukai, and M. Nakazawa, "10 Gbits/s soliton transmission over 2900 km using 1.3 μm singlemode fibres and dispersion compensation using chirped fibre Bragg gratings," Electron. Lett. **35**, 728–729 (1999).
8. P. Li, J. Shuisheng, Y. Fengping, N. Tigang, and W. Zhi, "Long-haul WDM system through conventional single mode optical fiber with dispersion compensation by chirped fiber Bragg grating," Opt. Commun. **222**, 169–178 (2003).
9. A. H. Gnauck, J. M. Wiesenfeld, L. D. Garrett, M. Eiselt, F. Forghieri, L. Arcangeli, B. Agogliata, V. Gusmeroli, and D. Scarano, "16 $\times$ 20 Gb/s, 400-km WDM transmission over NZDSF using a slope-compensating fiber-grating module," IEEE Photon. Technol. Lett. **12**, 437–439 (2000).
10. A. Sahara, T. Komukai, E. Yamada, and M. Nakazawa, "40 Gbits/s return-to-zero transmission over 500 km of standard fibre using chirped fibre Bragg gratings with small group delay ripples," Electron. Lett. **37**, 8–9 (2001).
11. F. Matera, V. Eramo, A. Schiffini, M. Guglielmucci, and M. Settembre, "Numerical investigation on design of wide geographical optical-transport networks based on $n \times 40$ Gb/s transmission," J. Lightwave Technol. **21**, 456–465 (2003).
12. N. J. Smith, F. M. Knox, N. J. Doran, K. J. Blow, and I. Bennion, "Enhanced power solitons in optical fibres with periodic dispersion management," Electron. Lett. **32**, 54–55 (1996).
13. J. H. B. Nijhof, W. Forysiak, and N. J. Doran, "The averaging method for finding exactly periodic dispersion-managed solitons," IEEE J. Sel. Top. Quantum Electron. **6**, 330–336 (2000).
14. A. Bondeson, M. Lisak, and D. Anderson, "Soliton perturbations—variational principle for the soliton parameters," Phys. Scr. **20**, 479–485 (1979).
15. P. T. Dinda, A. B. Moubissi, and K. Nakkeeran, "Collective variable theory for optical solitons in fibers," Phys. Rev. E **64**, 016608 (2001).
16. K. Nakkeeran, A. B. Moubissi, P. Tchofo Dinda, and S. Wabnitz, "Analytical method for designing dispersion-managed fiber systems," Opt. Lett. **26**, 1544–1546 (2001).
17. E. Poutrina and G. P. Agrawal, "Design rules for dispersion-managed soliton systems," Opt. Commun. **206**, 193–200 (2002).
18. K. Nakkeeran, Y. H. C. Kwan, and P. K. A. Wai, "Method to find the stationary solution parameters of chirped fiber grating compensated dispersion-managed fiber systems," Opt. Commun. **215**, 315–321 (2003).
19. K. Nakkeeran, A. B. Moubissi, and P. Tchofo Dinda, "Analytical design of dispersion-managed fiber system with map strength 1.65," Phys. Lett. A **308**, 417–425 (2003).
20. J. N. Kutz and P. K. A. Wai, "Ideal amplifier spacing for reduction of Gordon-Haus jitters in dispersion-managed soliton communications," Electron. Lett. **34**, 522–523 (1998).
21. T. Yu, E. A. Golovchenko, A. N. Pilipetskii, and C. R. Menyuk, "Dispersion-managed soliton interactions in optical fibers," Opt. Lett. **22**, 793–795 (1997).
22. A. Berntson, N. J. Doran, and J. H. B. Nijhof, "Power dependence of dispersion-managed solitons for anomalous, zero, and normal path-average dispersion," Opt. Lett. **23**, 900–902 (1998).
23. A. H. Liang, H. Toda, and A. Hasegawa, "High-speed soliton transmission in dense periodic fibers," Opt. Lett. **24**, 799–801 (1999).
24. S. K. Turitsyn, M. P. Fedoruk, and A. Gornakova, "Reduced-power optical solitons in fiber lines with short-scale dispersion management," Opt. Lett. **24**, 869–871 (1999).
25. L. J. Richardson, W. Forysiak, and N. J. Doran, "Dispersion-managed soliton propagation in short-period dispersion maps," Opt. Lett. **25**, 1010–1012 (2000).
26. A. B. Moubissi, K. Nakkeeran, P. Tchofo Dinda, and S. Wabnitz, "Average dispersion decreasing densely dispersion-managed fiber transmission systems," IEEE Photon. Technol. Lett. **14**, 1279–1281 (2002).
27. H. Chotard, Y. Painchaud, A. Mailloux, M. Morin, F. Trépanier, and M. Guy, "Group delay ripple of cascaded Bragg grating gain flattening filters," IEEE Photon. Technol. Lett. **14**, 1130–1132 (2002).
28. M. Ibsen and R. Feced, "Fiber Bragg gratings for pure

dispersion-slope compensation," Opt. Lett. **28**, 980–982 (2003).
29. A. K. Atieh, P. Myslinkski, J. Chrostowski, and P. Galko, "Measuring the Raman time constant (T_R) for soliton pulses in standard single-mode fiber," J. Lightwave Technol. **17**, 216–221 (1999).
30. P. T. Dinda, K. Nakkeeran, and A. Labruyére, "Suppression of soliton self-frequency shift by upshifted filtering," Opt. Lett. **27**, 382–384 (2002).
31. S. K. Turitsyn and V. K. Mezentsev, "Chirped solitons with strong confinement in transmission links with in-line fiber Bragg gratings," Opt. Lett. **23**, 600–602 (1998).